Fluorescence and morphology of self-assembled nucleobases and their diphenylalanine-hybrid aggregates

Concetta Avitabile[1], Carlo Diaferia[2], Valentina Roviello[3], Davide Altamura[4], Cinzia Giannini[4], Luigi Vitagliano[1], Antonella Accardo[2,*], Alessandra Romanelli[5,*]

[1]Institute of Biostructures and Bioimaging (CNR), via Mezzocannone 16, Naples (Italy)

[2]Department of Pharmacy, Research Centre on Bioactive Peptides (CIRPeB), University of Naples "Federico II", Via Mezzocannone 16, 80134, Naples, Italy

[3]Advanced Metrologic Service Center (CeSMA), University of Naples Federico II, Corso N. Protopisani, 80146 Naples, Italy.

[4]Institute of Crystallography (CNR), via Amendola 122, 70126 Bari (Italy)

[5]Department of Pharmaceutical Sciences, University of Milan, via Venezian 21, 20133 Milan (Italy)

Corresponding authors' e-mail:

alessandra.romanelli@unimi.it

antonella.accardo@unina.it

Abstract

Studies carried out in the last decades have unveiled that the ability to self-assemble is a widespread property among biomolecules. Small nucleic acid moieties or very short peptides are able to generate intricate assemblies endowed with remarkable structural and spectroscopic properties. Here we report structural/spectroscopic characterizations of aggregates formed by nucleobases as well as by Peptide Nucleic Acids (PNA)-peptide conjugates. At high concentration, all studied nucleobases form aggregates characterized by previously unreported fluorescence properties. The conjugation of these bases, as PNA derivatives, to the dipeptide Phe-Phe leads to the formation of novel hybrid assemblies, characterized by an amyloid-like association of the monomers. Although these compounds share the same basic cross-β motif, the nature and the number of PNA units have an important impact both on the level of structural order and on the intrinsic fluorescence of the self-assembled nanostructure.

Keywords: diphenylalanine, hybrid material, nucleobases, self-assembly

Introduction

The ability of nucleobases to self-assemble through hydrogen bonds and π-stacking is at the base of the formation of natural functional architectures that include duplex, triplex and quadruplex structures and of artificial supramolecular systems too, like DNA-origami.[1] Interactions between nucleobases have been also successfully exploited for the preparation of charge transfer complexes[2], non-linear optical single crystals[3] and nanomaterials.[4] The attachment of nucleobases to low molecular weight poly(tetrahydrofuran) produces materials showing high melting temperatures and mechanical stability;[5] chain-end conjugation of nucleobases to

oligomethylene results in the formation of hydrogels.[6] Hydrogen bond mediated pairing of nucleobases covalently linked to planar/aromatic molecules drives the formation of molecular cages or assemblies able to produce electron or energy transfer.[4a] Recently, it has been discovered that triphosphate nucleotides at low temperature and high concentration produce chromonic columnar liquid crystals, in which the bases are stacked and hydrogen bonded as in natural DNA duplexes[7].
Molecules containing both a peptide backbone and a nucleobase also show interesting properties: for example, nucleopeptides, composed of short homopeptides or heteropeptides conjugated to nucleobases, have been shown to self-assemble into supramolecular nanofibers and hydrogels too.[8] Recent studies demonstrate that Peptide Nucleic Acid (PNA) based molecules self-assemble to yield fluorescent aggregates.[9] For example, Guanine (g)-Cytosine (c) dimers produce voltage dependent electroluminescence as well as excitation dependent fluorescence in the visible range. Moreover, Fmoc-gc self-assembles at a very low concentration in organic solvents, to give fluorescent supramolecular structures characterized by a very high quantum yield in the visible range with lifetime in the nanosecond range.[10] These evidences make these compounds promising for development of novel optoelectronic materials. Fmoc/Bhoc protected PNA guanine monomers form uniform spherical assemblies, that arrange in a 2D periodic fashion as guanines on the skin of chameleons and respond with a color change to an increase in salt concentration.[11] PNA monomers, conjugated to peptides endowed with an alkyl tail, have been employed to produce fibers that further organize into supramolecular nanohelices; deposition of plasmonic nanoparticles onto fibers generates structures with plasmonic chirality with exceptional colloidal stability.[12]
The fluorescence of PNA aggregates has been supposed to depend on aggregation phenomena and seems to be related to the presence of nucleobases.
In 2012 Rapaport *et al.* reported the existence of aggregates formed by adenine and uracil after the observation of luminescence in 10^{-4} and 10^{-3} M solutions of the bases. [13] However, at the best of our knowledge, the ability of nucleobases to self-assemble in water and the optical properties of the resulting aggregates has never been investigated.
This work is aimed at filling this gap, by exploring the formation of nucleobases aggregates, their morphological features and their spectroscopic properties. The knowledge of these properties could be the starting point for the design of novel optoelectronic materials composed of natural building blocks. Furthermore, we explored the possibility to improve the aggregation ability of nucleobases by conjugating them, in the form of PNAs, to the diphenylalanine (FF) peptide, which is known to self-assemble into ordered structures.[14] Self-assembled aggregates of the hybrid molecules, formed by all monomers (a, c, g, t,) and homodimers (aa, cc, gg, tt) of PNA conjugated to FF, were fully characterized from the morphological and spectroscopic point of view.

Results and discussion

Studies on nucleobases have been carried out on thymine, cytosine and adenine. Due to solubility issues, the behavior of guanine cannot be investigated. For the three characterized nucleobases we detected the formation of aggregates by fluorescence. Indeed, all aggregates are fluorescent, emitting between 370 and 400 nm (Figure 1, Table S1). Aggregates of adenine and thymine show Stokes' shifts of about 80 nm and an increase in the emission wavelength at increasing excitation wavelength (REES) (Figure S1). This phenomenon has been already observed for aggregates formed by PNAs and was attributed to the interactions of aggregates with solvents.[9-10] Cytosine aggregates instead show a 40 nm Stokes shift and no REES, suggesting a different polarity of the aggregates. The shift of the absorption peak toward higher wavelengths, the sharpening of the peaks observed for the aggregates compared to monomeric species, as well as the fluorescence of the samples, suggest the formation of J-type aggregates in all cases.[15] These analyses were performed either using fresh solutions of bases in water or using solutions subjected to an annealing process (i.e. warming up to 90°C and slowly cooling down to 4°C), which is commonly employed when oligonucleotide hybrids, such as duplexes, have to be formed in order to produce the thermodynamically stable structure. Results obtained using the two different protocols are

superimposable, suggesting that the organization of the nucleotides into aggregates is a fast process. In order to investigate the self-assembling properties of nucleobases, we quantitatively estimated their critical aggregation concentration (CAC) values by a fluorescence-based method using 8-anilinonaphthalene-1-sulfonate ammonium salt (ANS) as a polarity sensitive probe. ANS fluorophore does not show fluorescence emission in hydrophilic environment. By contrast, the fluorescence emission increases dramatically in the range of 465-480 nm in hydrophobic environment (*e.g.* in the inner micellar compartment or aromatic spine of peptide aggregates).[16] The analytical determination of the CAC values for nucleobases was assessed titrating a 200 μM ANS solution with growing amounts of nucleobase solutions and extrapolated in the break-point of the concentration *vs* emission graph (Figure S2a). Since ANS is a planar aromatic molecule, in principle, it might interact by stacking with nucleobases, thus interfering with the self-assembling and yielding erroneous results in term of CAC calculation. For this reason, taking advantage of the fluorescence of the aggregates, CACs were also determined measuring the fluorescence of nucleobase aggregates as a function of their concentration (Figure S2b). As reported in Table 1, CACs obtained by ANS and direct titrations, are comparable only for thymine, suggesting an interaction between ANS and cytosine or adenine. In all cases, CACs are in the millimolar range. Fluorescence microscopy analysis of samples drop-casted and air-dried on a glass slide reveals the ability of all bases to emit in the blue and in the green spectral regions. Deposition of nucleobases on the glass results in formation of crystals for thymine and cytosine (Figure 1 and S3). Indeed, SEM observations reveal the formation of plate-like crystals for cytosine, flower-like crystals for adenine and amorphous structures for thymine (Figure 1). Other attempts, performed either by CD or by WAXS/GIWAXS analyses to gain information on the structure of nucleobases into the aggregates failed, probably due to an intrinsic instability of the aggregates.

The observation that individual bases possess an intrinsic propensity to form aggregates with interesting spectroscopic properties prompted us to conjugate them with self-assembling systems to check both the structural and spectroscopic features of the resulting compounds. Specifically, we used as self-assembling motif the well-known ultrashort aggregative system Phe-Phe (FF). This aromatic dipeptide is able to self-assemble with a high morphological variability depending on the experimental conditions.[17] Recently, the ability of Boc and Fmoc protected Phe-Phe conjugated to the nucleoside adenine to form spherical aggregates has been reported.[18] We decided to use PNAs as source of nucleobases, as these are very easy to manage and to conjugate to peptides. Aggregation of the PNA monomers and dimers has been already investigated; it has been found that only in alkaline conditions the gg, gc and cg dimers self-assemble, unlike all the other combination of bases.[9] In addition, aggregates are observed for Fmoc-g(Bhoc)-OH. On the other hand, PNA monomers lacking protecting groups on the exocyclic amines of nucleobases and on the amino-terminus do not aggregate. This behavior may be due to the intrinsic flexibility of the PNA backbone, that hampers the self-assembly of the free monomers.

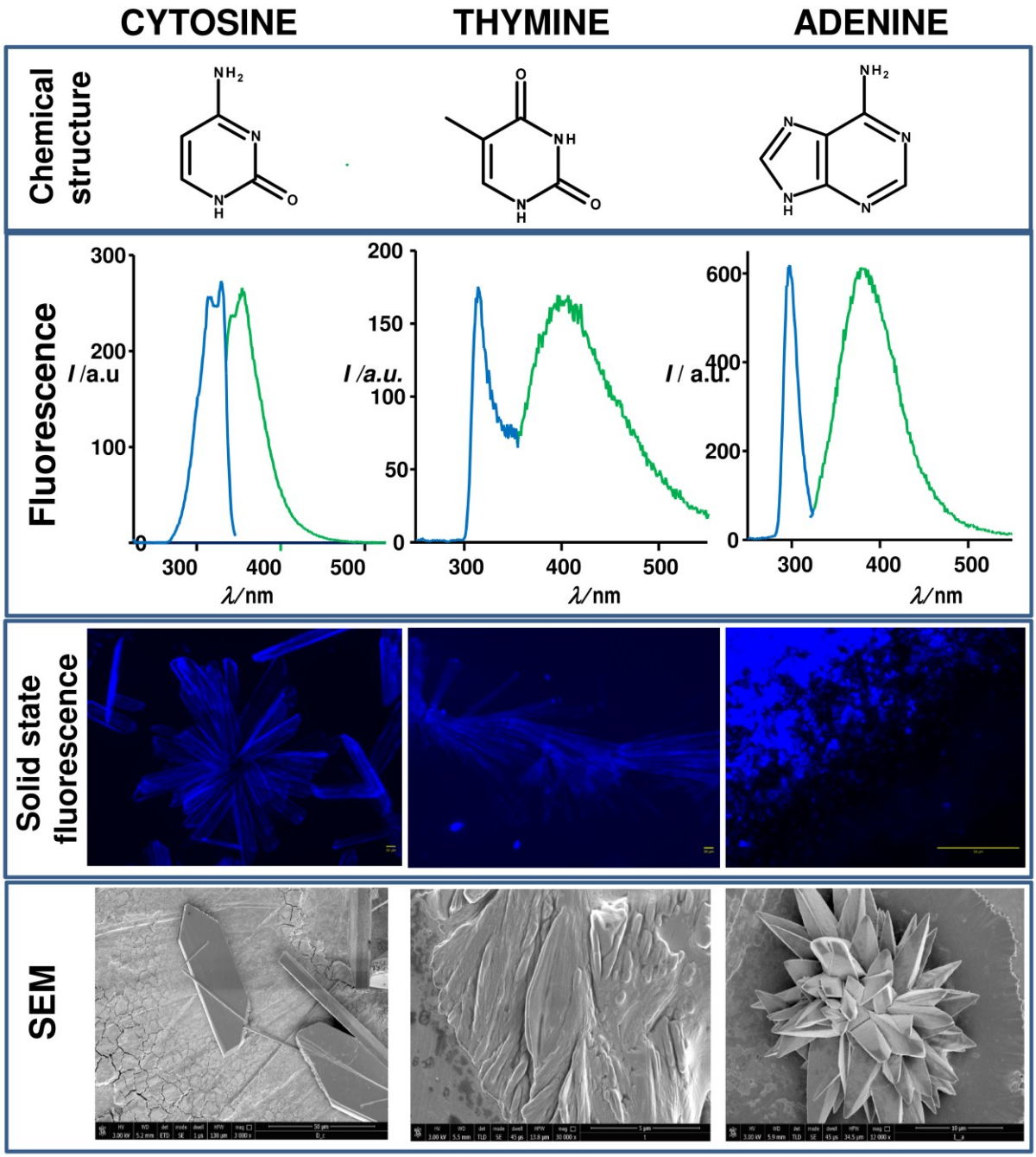

Figure 1. I row: chemical structure of the nucleobases; II row excitation and emission spectra for nucleobases in water in aggregated form. For cytosine λ_{ex}: 320 nm, λ_{em}: 380 nm; for thymine λ_{ex}: 310 nm, λ_{em}: 396; for adenine λ_{ex}: 300 nm, λ_{em}: 380 nm. Spectra were recorded in water at a concentration of 8.0 mg/mL for cytosine, 20 mg/mL for thymine and 3.5 mg/mL for adenine. III row: Fluorescence microscopy images of nucleobases aggregates drop-casted on glass slides and air-dried at room temperature. Images were obtained by exciting the samples in DAPI (λ_{ex}=359 nm, λ_{em}=461 nm) spectral region. The scale bar is 200 μm for cytosine and thymine, and 50 μm for adenine. IV row: Selected SEM micrographs collected for the nucleobases: cytosine (3000x, 50μm scale bar), thymine (30000x, 5μm scale bar) and adenine (12000x, 10μm scale bar).

Table 1: Comparison between CAC values obtained for nucleobases in presence or in absence of ANS fluorophore (*if*: intrinsic fluorescence).

Nucleobase	CAC (ANS) (mM)	CAC (*if*) (mM)
Thymine	42.7	20.0
Adenine	39.8	1.05
Cytosine	0.501	0.064

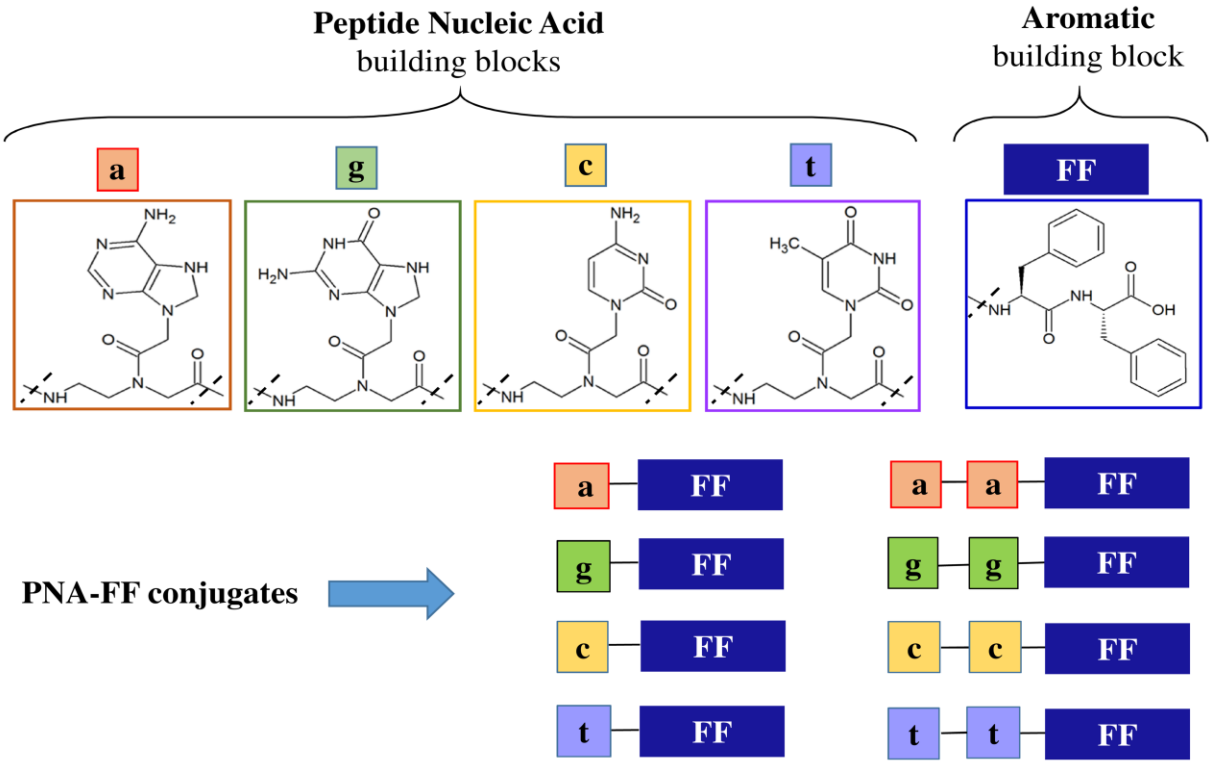

Figure 2: The eight hybrid conjugates are composed of one or two PNA residues (adenine, *a*; guanine, *g*; cytosine, *c*; thymine, *t*) covalently bound at the N^{α}-terminus of the diphenylalanine aromatic homodimer (FF).

We investigated conjugates of FF to PNA monomers and dimers. PNA-FF derivatives, depicted in Figure 2, were synthesized by solid phase according to Fmoc strategy (see Supplementary Materials for experimental details and characterization of peptide derivatives in Figure S4-S7 and in Table S2 and S3).[19] All the PNA-FF derivatives contain the FF moiety at the C-terminus of PNAs. All the PNA-FF conjugates show a good solubility in water (up to 20 $mg \cdot mL^{-1}$). Importantly, upon conjugation to diphenylalanine we were able to investigate also aggregates formed by guanine. Due to the coexistence of two potential aggregative motives in these hybrids (FF dipeptide and the nucleobase), it is intriguing to figure out which moiety directs the final structure of the aggregates and which dictates the spectroscopic properties.

As expected, conjugates of PNAs to FF show CAC lower as compared to free nucleobases. When two PNA bases are connected to FF, the CAC is lower than that observed for a single PNA base bound to FF (Table 2, Figures 3a,3b and S8). These results suggest that the additional π-π stacking due to the phenyl groups in the diphenylalanine triggers the aggregation of nucleobases, suggesting a possible cooperative effect between nucleobase and FF-homodimer. According to this hypothesis, all the PNA-FF conjugates containing two nucleobases exhibit a lower CAC value. This effect is more striking for the pyrimidine conjugates and likely depends on the lower steric hindrance of these bases that result in a better ability to pack with each other.We then characterized the structural

properties of these aggregates using a repertoire of experimental techniques. In order to determine the secondary structure of PNA-FF aggregates in solution, we performed Circular Dichroism (CD) and Fourier Transform Infrared (FTIR) experiments (Figures 3c, S9-S10).

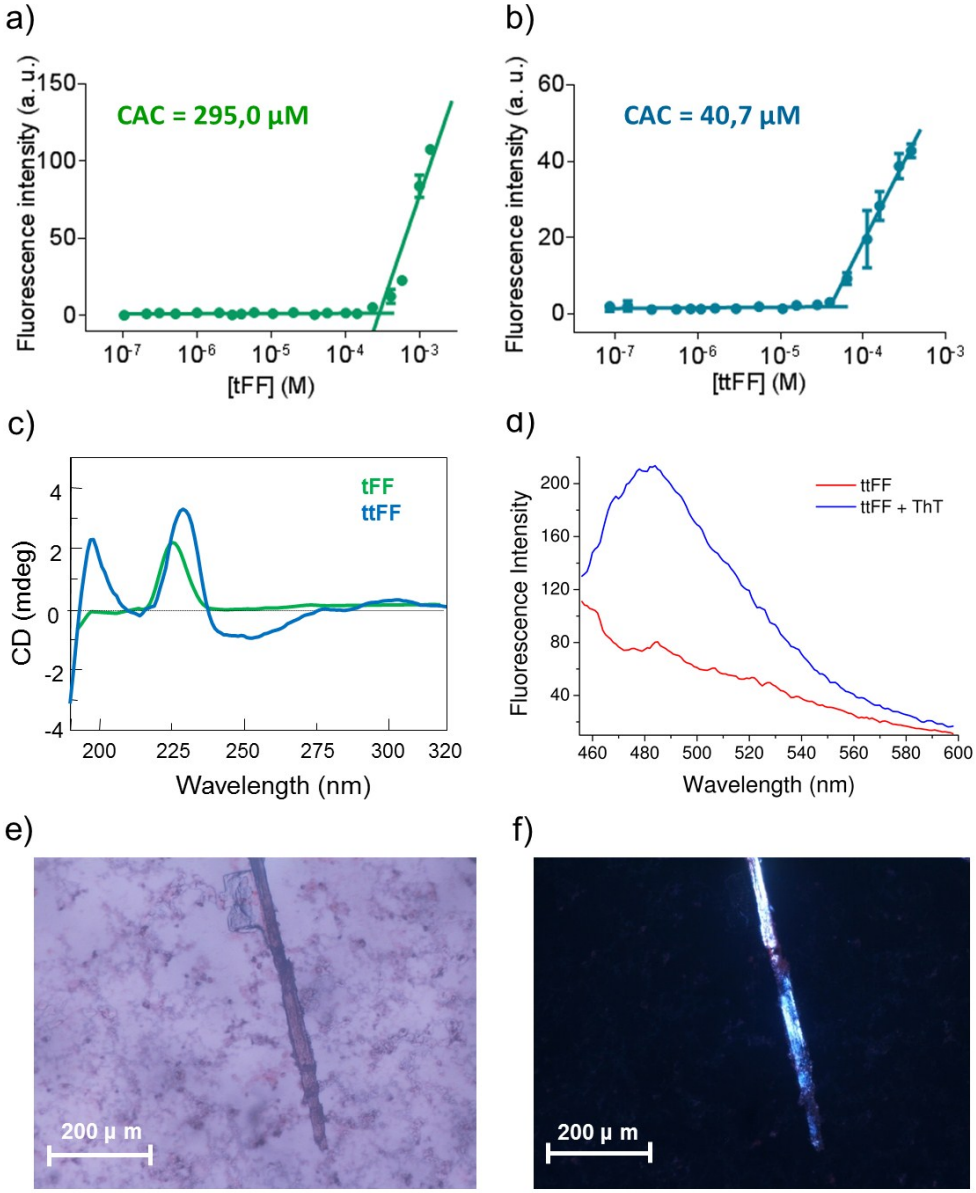

Figure 3: CAC determination and secondary stucture characterization for self-assembled aggregates of tFF and ttFF conjugates. Plots of the fluorescence intensity emission of ANS fluorophore at 470 nm *vs.* concentration of the tFF (a) and ttFF (b) conjugates for the CAC determination. c) CD spectra of tFF and ttFF conjugates in aqueous solution at a concentration of 20 $mg \cdot mL^{-1}$. d) Fluorescence spectra of ThT before and immediately after the addition of ttFF derivative in water at a final concentration of 5.0 $mg \cdot mL^{-1}$ in cuvette. Polarized optical microscopy images of air-dried ttFF sample stained with Congo Red solution under bright-field illumination (e) and between crossed polars (f).

Table 2: CAC values for all the PNA-FF (X-FF) conjugates reported in μM ($mg \cdot mL^{-1}$)

X	a	g	c	t
X-FF	114.8 (0.0669)	162.2 (0.0978)	117.4 (0.0660)	295.0 (0.170)
XX-FF	91.20 (0.0786)	138.0 (0.123)	41.70 (0.0340)	40.70 (0.0343)

All CD spectra show a maximum around 225 nm; this signal is diagnostic of Phe-Phe in its aggregated form (Figure 3c and S9).[20] Signals appearing around 250 nm in spectra of ttFF and aaFF may be indicative of stacking between bases.[21] The occurrence of β-sheet formation was also confirmed by FTIR spectroscopy in the amide I spectral region (1600-1700 cm^{-1}). Deconvolution in absorbance for the secondary structure prediction of the FTIR spectra is reported in Figure S10. The appearance of two peaks around 1640 and 1680 cm^{-1} in aggregates formed by tFF and cFF supports the hypothesis of antiparallel stacks. Similar results have been reported in the literature for hexaphenylalanine aggregates.[22] On the other hand, the profiles observed for the other samples are characterized by a very large band with a maximum at 1640 cm^{-1}. In these cases it is possible that residual TFA concurs to the broadening of the signals. A comparative analysis of these FTIR data suggests that the size of the bases of the PNA moiety has a significant impact on the structure of the basic motif of these aggregates. Indeed, conjugation of PNAs containing a single pyrimidine base does not influence the aggregation mode of the FF moiety, whereas PNAs embodying a single purine lead to a partial disorganization of the antiparallel β-sheet aggregation. It is likely that the ability of purine bases to form stronger stacking interactions somehow perturbs the motif detected in FF-based compounds. In line with these considerations, the conjugation of PNAs containing more than one base has perturbative effects on the antiparallel association mode of the basic units of these assemblies. β-sheet structure was further confirmed by using the Thioflavin T (ThT) spectroscopic assay. Fluorescence spectra of PNA-peptides recorded either before or after the addition of the ThT, are reported in Figures 3d and S11. The rapid appearance of an emission peak at 482 nm after the addition of ThT indicates the binding of the ThT to the peptide derivative[23]. The fluorescence signal for all the samples remains unvaried until 2 hours from the incubation of ThT with the peptide solution. This result confirms the occurrence of a very fast aggregation kinetic for PNA-FF in water.

Nanostructures obtained by self-assembly of PNA-FF constructs were also characterized at the solid state by SEM and WAXS/GIWAXS measurements (Figure 4). Conjugation of FF to nucleobases deeply affects the morphology of the aggregates. SEM micrographs of FF-conjugates containing one monomer of adenine, aFF, show the formation of amorphous conglomerates at the nanometric scale with a surface rich in small spheroids (Figure S12). On the contrary, SEM micrographs of FF-derivative containing a dimer of adenine, aaFF exhibit fibrous nanostructures. Similar behaviour was observed for gFF and ggFF. (Figure S13). SEM microphotos of all the FF-conjugates containing monomers or dimers of pyrimidine bases show entwined fibres with a mean length of 250 μm and a thickness of 15-20 μm (Figure 4 and S14 and S15).

A deep characterization of the nanostructures was performed by WAXS and GIWAXS scattering techniques in transmission and reflection mode, respectively. GIWAXS diffraction patterns have been collected on the PNA-FF conjugates deposited onto Si substrates. All samples present a major peak at ~ 4.5-4.8 Å that is indicative of the β-sheet structure of the aggregates. A deeper inspection of the diffraction pattern highlights some interesting specificities among the investigated samples. Indeed, only tFF and ttFF present a minor peak at lower resolution (12.5 – 13.0 Å) (Figure 4a and Table S4). This peak has been frequently found in assemblies formed by Phe-containing peptides

and has been attributed to the lateral packing of the Phe side chains located at the inter-sheet interface.[24] The presence of this peak in tFF and ttFF and its absence in the other systems suggests that these compounds present a different level of structural organization in which the FF moiety has a major role in the supramolecular structuration. In the other compounds, the ability of the bases to be involved in stronger interactions produces a significant perturbation in the FF association by preventing regularities in the packing of the Phe side-chains. In this framework, it is interesting to note that a closer analysis of the tFF and ttFF shows that the peak at 12.5 – 13.0 Å is sharper in former compounds. In line with our interpretation, the presence of a single thymine base has less perturbative effects on the Phe-association. Several attempts were made to generate air-dried fibers suitable for WAXS studies using the stretch frame method.[25] Only for thymine containing conjugates (tFF and ttFF), we were able to prepare elongated structures that were approximately 0.5 mm long (Figure S16). The WAXS analysis of these samples, however, produced diffraction patterns characterized by rings (Figure S16). This finding indicates that these samples present a powder-like macroscopic structural order of the fiber. Nevertheless, the spacing of these rings (Figure S16 and Table S5) is clearly indicative of the cross-β structure of these assemblies highlighted by the GIWAXS data. The self-organization of PNA-FF conjugates in β-sheet structure was also evaluated by Congo Red (CR) birefringence assay (Fig. 3e,f)[26] All the PNA-FF conjugates, drop-casted on the glass slide and stained with CR, exhibit intense green birefringence when imaged with polarized optical microscopy, thus confirming the presence of the cross-β structure

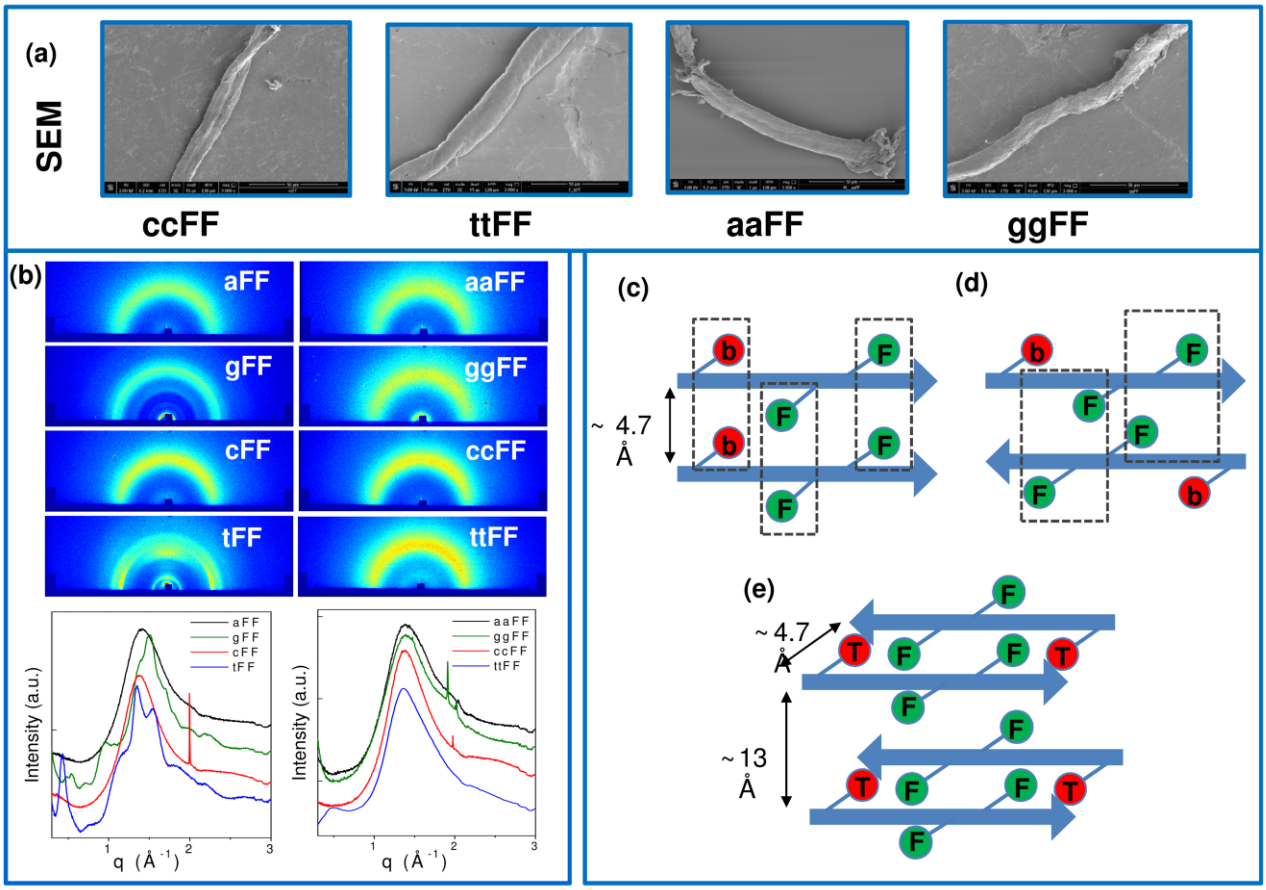

Figure 4: a) Selected SEM micrographs collected for aaFF, ttFF, aaFF and ggFF PNA-FF derivatives. Magnification and scale bar for all samples are 3000x, 50µm, respectively. b) 2D GIWAXS data (upper part) and the corresponding 1D profiles (lower part) of PNA-FF conjugates as deposited onto Si substrates; c) Schematic representation of the possible intra-sheet and inter-sheet association modes of PNA-FF β-strands. c) and d) Schematic representation of the parallel

and antiparallel associations of the β-strands within a single β-sheet, respectively. Letter "b" and "**F**" is a generic notation for the base and for the phenylalanine, respectively. e) The association of two β-sheets, each made of antiparallel β-strands, is shown for the conjugate tFF. The value of the repetitive intra-sheet and inter-sheet spacing is also reported.

The characterization of these compounds provides interesting insights into the role played by the different interactions (H-bonding and hydrophobic/stacking interactions) in dictating the structure of these assemblies. In contrast to FF, which forms nanotubular structures, the conjugates here designed and characterized assume cross-β structures that are somehow modulated by the nature and by the number of bases attached to the FF moiety. The inspection of the very simple motif of these β structures, *i.e.* the assertion modes of the β-strands, indicates that intrinsic preference of Phe-rich peptides to antiparallel sheet is perturbed by the presence of single PNA bearing a purine base or of a PNA-dimer. As schematically shown in Figure 4b, the parallel association of the strands favours base-base interactions that somehow compete with the factors, which favour the antiparallel state.[22] As a result of these competing factors, only tFF and cFF present a uniform antiparallel state, whereas the others are likely made of a mixture of parallel and antiparallel state (Figure 4b,c). This is in line with the observation that pyrimidine-pyrimidine stacking associations are weaker than purine-purine ones.[27] The analysis of the structure of the assemblies formed by these conjugates indicates that the presence of the PNAs tends to reduce the lateral order of these aggregates when compared to those observed in Phe-rich peptide. Once again, the possibility of the bases to form alternative interactions prevents the formation of repetitive interactions between Phe-side chains. This is consistent with the observation that individual bases can establish a wide range of interactions at solid state.[28] With the exception of tFF and, at minor extent, of ttFF, all these compounds display cross-β structures that are not stabilized by a precise lateral packing.

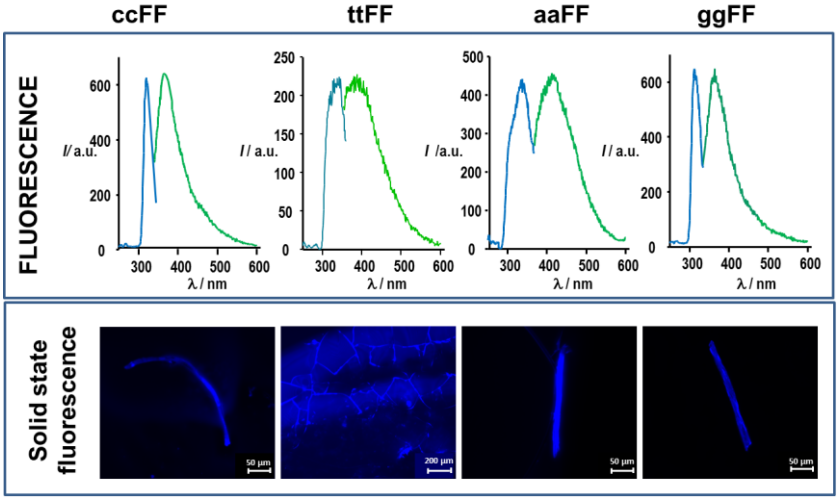

Figure 5: Top panel: Excitation and emission spectra for PNA-FF conjugates in water. For ccFF λ_{ex}: 320 nm, λ_{em}: 364 nm; for ttFF λ_{ex}: 330 nm, λ_{em}: 390; for aaFF λ_{ex}: 340 nm, λ_{em}: 420 nm, for ggFF λ_{ex}: 310 nm, λ_{em}: 375 nm. Bottom panel: Fluorescence microscopy images of FF-PNA aggregates drop-casted on glass slides and air-dried at room temperature. Images were obtained by exciting the samples in DAPI (λ_{ex}=359 nm, λ_{em}=461 nm) spectral region. The scale bar is 200 μm for ttFF, and 50 μm for ccFF, aaFF, ggFF.

The analysis of the spectroscopic properties of these compounds, which present a radically different structure compared to the individual nucleobases, highlights the occurrence of significant fluorescence signals (Figure 5,Table S1). Moreover, aggregates formed by conjugates of PNA to FF show fluorescence properties in solution and their emission/excitation spectra are reported in Figure 5, S17 and S18. The fluorescence properties of the aggregates seem in all cases to be dictated by the

nucleobases although their Phe-Phe moiety drives their cross-β structure. Indeed, no emission is observed upon excitation at 257 nm, which corresponds to the excitation wavelength of FF in various morphologies.[29] As previously observed for self-assembled nucleobases, all the PNA-FF conjugates exhibit an emission peak around 380-400 nm when excited at 310 nm. In the spectra of the adenine-based conjugates, a significant red shift of both the excitation and emission wavelengths (λ_{exc}= 340 nm and λ_{em}= 420 nm) can be observed. Collectively, these findings suggest that the nucleobases are able to establish tight interactions in these amyloid-like assemblies. Beside the maximum attributable to the PNA aggregation, spectra of pyrimidine conjugates exhibit an additional maximum at 460 nm when excited around 370 nm (Figure S19). This latter peak is typically observed in fibrillary amyloid-like nanostructures rich in β-sheet assemblies.[23a] In the compound tFF this signal is evident (Figure 6). This spectroscopic behavior is in line with the structural features above described. Immunofluorescence images in Figure S20 indicate the capability of supramolecular structures to keep their fluorescence properties also at the solid-state for samples drop-casted on glass. Preliminary spectroscopic studies were also performed for FF conjugates in methanol, in order to understand whether the aggregation, fluorescence and conformational properties of our compounds could be modified by changing the polarity of the environment. In the literature, in fact, it is reported that the amphiphile diphenylalanine derivative TFA-FF-OBzl adopts different structures according to the polarity of the environment.[30] Fluorescence properties, as well as CD signature in methanol and in water are very similar (TableS1b, Figures S21 and S22), suggesting that, in the experimental conditions that were investigated, the supramolecular organization is the same.

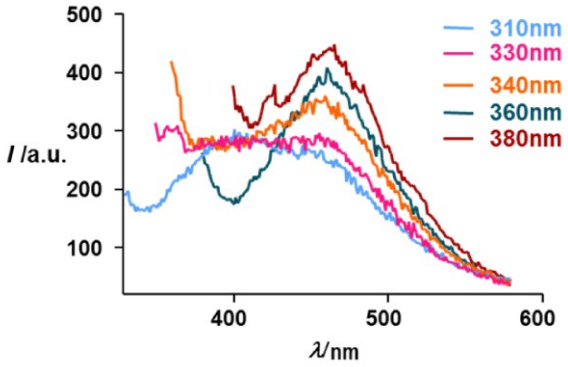

Figure 6: Fluorescence spectra of tFF in water at different excitation wavelength; the maximum at 470 nm is diagnostic of the β-sheet structure of the assembly.

Conclusions

Structural studies highlighted the capability of water-soluble nucleobases (adenine, thymine and cytosine) to self-assemble in well-organized super structures above a critical concentration value. In their aggregated form, they show different spectroscopic behaviour with a substantial red shift of the absorbance peak and the appearance of unexpected fluorescence around 370-400 nm upon excitation at 310 nm. The conjugation of one or two PNA monomers to well-known aggregating motif FF peptide improves their tendency to self-assemble as suggested by the decrease of CAC. After the conjugation, the morphology of the PNA-FF aggregates is the result of a delicate balance of different factors. A full understanding of the role that different interactions play in these systems is important for the development of new biomaterials based on these conjugates. The structural characterizations of self-assembled, hybrid PNA-FF conjugates demonstrate that in these compounds the FF moiety drives the aggregation process. Beside π-π stacking between the phenyl rings, hydrogen bonds between PNA can occur. However, these latter are strongly determined by

the nature (purine or pyrimidine) and the number of bases. It is worth to note that although the overall structural features of the aggregates are directed by the FF moiety, bases are still able to interact and to form systems with intriguing spectroscopic features. Importantly, the ability of these compounds to aggregate in organic solvents and in water allows possible applications in different fields, ranging from the biomedical to technological areas.

Acknowledgments

Teresa Sibillano is acknowledged for collection of the WAXS data and Rocco Lassandro for technical support in the XMI-L@b. AA and CD acknowledge the financed project POR CAMPANIA FESR 2014/2020.

References

[1] a) P. F. Wang, T. A. Meyer, V. Pan, P. K. Dutta and Y. G. Ke, *Chem* **2017**, *2*, 359-382; b) A. Levy-Lior, E. Shimoni, O. Schwartz, E. Gavish-Regev, D. Oron, G. Oxford, S. Weiner and L. Addadi, *Advanced Functional Materials* **2010**, *20*, 320-329.

[2] a) T. Murata, Y. Enomoto and G. Saito, *Solid State Sciences* **2008**, *10*, 1364-1368; b) O. Neilands, *Molecular Crystals and Liquid Crystals* **2001**, *355*, 331-349.

[3] P. Jaikumar, S. Sathiskumar, T. Balakrishnan and K. Ramamurthi, *Materials Research Bulletin* **2016**, *78*, 96-102.

[4] a) J. L. Sessler, C. M. Lawrence and J. Jayawickramarajah, *Chemical Society Reviews* **2007**, *36*, 314-325; b) S. Sivakova and S. J. Rowan, *Chemical Society Reviews* **2005**, *34*, 9-21; c) S. Romero-Perez, J. Camacho-Garcia, C. Montoro-Garcia, A. M. Lopez-Perez, A. Sanz, M. J. Mayoral and D. Gonzalez-Rodriguez, *Organic Letters* **2015**, *17*, 2664-2667; d) C. Montoro-Garcia, J. Camacho-Garcia, A. M. Lopez-Perez, N. Bilbao, S. Romero-Perez, M. J. Mayoral and D. Gonzalez-Rodriguez, *Angewandte Chemie-International Edition* **2015**, *54*, 6780-6784.

[5] S. J. Rowan, P. Suwanmala and S. Sivakova, *Journal of Polymer Science Part a-Polymer Chemistry* **2003**, *41*, 3589-3596.

[6] R. Iwaura, K. Yoshida, M. Masuda, K. Yase and T. Shimizu, *Chemistry of Materials* **2002**, *14*, 3047-3053.

[7] G. P. Smith, T. P. Fraccia, M. Todisco, G. Zanchetta, C. H. Zhu, E. Hayden, T. Bellini and N. A. Clark, *Proceedings of the National Academy of Sciences of the United States of America* **2018**, *115*, E7658-E7664.

[8] a) X. M. Li, Y. Kuang, H. C. Lin, Y. Gao, J. F. Shi and B. Xu, *Angewandte Chemie-International Edition* **2011**, *50*, 9365-9369; b) D. Yuan, X. W. Du, J. F. Shi, N. Zhou, J. Zhou and B. Xu, *Angewandte Chemie-International Edition* **2015**, *54*, 5705-5708.

[9] O. Berger, L. Adler-Abramovich, M. Levy-Sakin, A. Grunwald, Y. Liebes-Peer, M. Bachar, L. Buzhansky, E. Mossou, V. T. Forsyth, T. Schwartz, Y. Ebenstein, F. Frolow, L. J. W. Shimon, F. Patolsky and E. Gazit, *Nature Nanotechnology* **2015**, *10*, 353-360.

[10] C. Avitabile, C. Diaferia, B. Della Ventura, F. A. Mercurio, M. Leone, V. Roviello, M. Saviano, R. Velotta, G. Morelli, A. Accardo and A. Romanelli, *Chemistry* **2018**, *24*, 4729-4735.

[11] O. Berger, E. Yoskovitz, L. Adler-Abramovich and E. Gazit, *Advanced Materials* **2016**, *28*, 2195-2200.

[12] Y. Lin, E. T. Pashuck, M. R. Thomas, N. Amdursky, S. T. Wang, L. W. Chow and M. M. Stevens, *Angewandte Chemie* **2017**, *56*, 2361-2365.

[13] V. L. Rapoport, V. M. Malkin, A. V. Savina, E. A. Safargaleeva and V. V. Goriuchko, *Biofizika* **2012**, *57*, 14-20.

[14] X. H. Yan, P. L. Zhu and J. B. Li, *Chemical Society Reviews* **2010**, *39*, 1877-1890.

[15] F. Wurthner, T. E. Kaiser and C. R. Saha-Moller, *Angewandte Chemie-International Edition* **2011**, *50*, 3376-3410.

[16] a) A. Accardo, A. Morisco, P. Palladino, R. Palumbo, D. Tesauro and G. Morelli, *Molecular bioSystems* **2011**, *7*, 862-870; b) C. Diaferia, E. Gianolio, T. Sibillano, F. A. Mercurio, M. Leone, C. Giannini, N. Balasco, L. Vitagliano, G. Morelli and A. Accardo, *Scientific reports* **2017**, *7*, 307; c) C. Diaferia, T. Sibillano, D. Altamura, V. Roviello, L. Vitagliano, C. Giannini, G. Morelli and A. Accardo, *Chemistry* **2017**, *23*, 14039-14048.

[17] S. Marchesan, A. V. Vargiu and K. E. Styan, *Molecules* **2015**, *20*, 19775-19788.
[18] D. Datta, O. Tiwari and K. N. Ganesh, *Nanoscale* **2018**, *10*, 3212-3224.
[19] a) C. Avitabile, L. Moggio, L. D. D'Andrea, C. Pedone and A. Romanelli, *Tetrahedron Letters* **2010**, *51*, 3716-3718; b) C. Avitabile, L. Moggio, G. Malgieri, D. Capasso, S. Di Gaetano, M. Saviano, C. Pedone and A. Romanelli, *PloS one* **2012**, *7*.
[20] N. Amdursky and M. M. Stevens, *Chemphyschem : a European journal of chemical physics and physical chemistry* **2015**, *16*, 2768-2774.
[21] V. A. Bloomfield, D. M. Crothers and I. Tinoco, **2000**, p. .
[22] C. Diaferia, T. Sibillano, D. Altamura, V. Roviello, L. Vitagliano, C. Giannini, G. Morelli and A. Accardo, *Chemistry-a European Journal* **2017**, *23*, 14039-14048.
[23] H. LeVine, 3rd, *Protein science : a publication of the Protein Society* **1993**, *2*, 404-410.
[24] a) C. Diaferia, T. Sibillano, N. Balasco, C. Giannini, V. Roviello, L. Vitagliano, G. Morelli and A. Accardo, *Chemistry-a European Journal* **2016**, *22*, 16586-16597; b) C. Diaferia, T. Sibillano, C. Giannini, V. Roviello, L. Vitagliano, G. Morelli and A. Accardo, *Chemistry* **2017**, *23*, 8741-8748.
[25] M. Sunde, L. C. Serpell, M. Bartlam, P. E. Fraser, M. B. Pepys and C. C. F. Blake, *Journal of Molecular Biology* **1997**, *273*, 729-739.
[26] a) W. E. Klunk, R. F. Jacob and R. P. Mason, *Analytical biochemistry* **1999**, *266*, 66-76; b) C. Diaferia, E. Gianolio, P. Palladino, F. Arena, C. Boffa, G. Morelli and A. Accardo, *Advanced Functional Materials* **2015**, *25*, 7003-7016.
[27] R. A. Friedman and B. Honig, *Biophysical Journal* **1995**, *69*, 1528-1535.
[28] a) K. Hoxha, D. H. Case, G. M. Day and T. J. Prior, *Crystengcomm* **2015**, *17*, 7130-7141; b) T. Stolar, S. Lukin, J. Pozar, M. Rubcic, G. M. Day, I. Biljan, D. S. Jung, G. Horvat, K. Uzarevic, E. Mestrovic and I. Halasz, *Crystal Growth & Design* **2016**, *16*, 3262-3270; c) K. Ozeki, N. Sakabe and J. Tanaka, *Acta Crystallographica-Section B* **1969**, *825*, 1038-1045.
[29] Z. X. Gan and H. Xu, *Macromolecular Rapid Communications* **2017**, *38*.
[30] E. Mayans, G. Ballano, J. Sendros, M. Font-Bardia, J. L. Campos, J. Puiggali, C. Cativiela and C. Aleman, *Chemphyschem : a European journal of chemical physics and physical chemistry* **2017**, *18*, 1888-1896.

Table of Contents

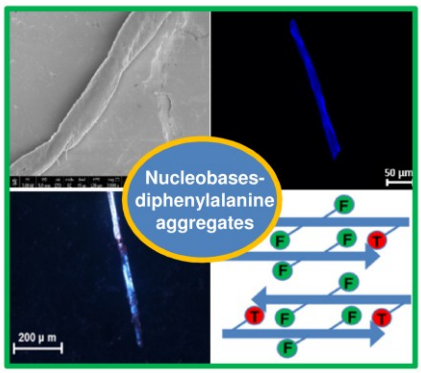

Natural nucleobases aggregate in water and emit fluorescence. When nucleobases within a Peptide Nucleic Acid backbone are conjugated at the N-terminus of Phe-Phe, aggregation occurs at lower concentrations. In the PNA-Phe-Phe conjugates, the Phe-Phe moiety directs formation of antiparallel stacks that show fluorescence either in solution and at the solid state.